

The Spin-Kinetic Temperature Coupling and the Heating Rate due to Lyman Alpha Scattering before Reionization: Predictions for 21cm Emission and Absorption

Xuelei Chen

The Kavli Institute for Theoretical Physics, UCSB, Santa Barbara, CA 93106, USA

xuelei@kitp.ucsbs.edu

and

Jordi Miralda-Escudé

Department of Astronomy, The Ohio State University, Columbus, OH 43210, USA

jordi@astronomy.ohio-state.edu

ABSTRACT

We investigate the interaction of Ly α photons produced by the first stars in the universe with intergalactic hydrogen prior to reionization. The background Ly α spectral profile is obtained by solving a Fokker-Planck equation. Accurate values of the heating and scattering rates, and the spin-kinetic temperature coupling coefficient, are presented. We show that the heating rate induced by the Ly α scatterings is much lower than found previously, and is basically negligible. The dominant heating source is most likely the X-rays from the first ionizing sources, which are able to penetrate into the atomic medium. The scattering of Ly α photons couples the hydrogen spin temperature to the kinetic temperature. If the first ionizing sources in the universe did not emit significant X-rays, the spin temperature would be rapidly brought down to the very low gas kinetic temperature, and a 21cm absorption signal against the CMB larger than 100 mK would be predicted. However, we argue that sufficient X-rays are likely to have been emitted by the first stellar population, implying that the gas kinetic temperature should rapidly increase, turning a reduced and brief absorption signal into emission, with a smaller amplitude of ~ 10 mK. The detection of the 21cm absorption and emission feature would be a hallmark in unravelling the history of the “dark age” before reionization.

Subject headings: cosmology: theory — diffuse radiation — cosmic microwave background — intergalactic medium — line: formation — radio lines: general

1. Introduction

After recombination of the primordial plasma at $z \sim 1000$, the Universe entered an age of darkness. The primordial density fluctuations continued to grow, until non-linear gravitational collapse led to the formation of the first dark matter halos in which the gas could collapse, and then radiatively cool. The dark ages ended at the time when the first stars formed in these halos, with a characteristic mass of $\sim 10^6 M_\odot$ (Couchman & Rees 1986; Tegmark et al. 1997; Abel et al. 2000; Bromm et al. 2002). These first stars, as well as any black holes or neutron stars formed subsequently which could accrete surrounding matter, produced photons capable of ionizing hydrogen (with wavelength $\lambda < 91.2 \text{ nm}$). As soon as the ionizing radiation produced in the sites of star formation was able to escape into the low-density intergalactic medium, the process of reionization started. During reionization, the ionized volume fraction of the universe increased gradually, until all the low-density regions were ionized. Recent observations of the Gunn-Peterson trough (Gunn & Peterson 1965) at $z \gtrsim 6$ (Becker et al. 2001; Fan et al. 2002, 2003), indicate that the end of reionization probably occurred at $z \simeq 6$, although the epoch at which reionization began is still unknown (e.g., Gnedin 2000; Miralda-Escudé 2003).

The redshifted 21 cm line opens up a promising window for observing this period of cosmic history. This line is produced by the transition between the singlet and triplet hyperfine levels of the hydrogen atom at the electronic ground state. The line can be observed in absorption or emission against the Cosmic Microwave Background (CMB). The brightness temperature is given by

$$\delta T = \frac{T_s - T_{CMB}}{1 + z} (1 - e^{-\tau}) \simeq (0.025 \text{ K}) \left(\frac{\Omega_b h_0}{0.03} \right) \left(\frac{0.3}{\Omega_{m0}} \right)^{1/2} \left(\frac{1 + z}{10} \right)^{1/2} \frac{\rho_{HI}}{\bar{\rho}_H} \frac{T_s - T_{CMB}}{T_s}. \quad (1)$$

where T_s and T_{CMB} are the hydrogen spin temperature and the CMB temperature, τ is the optical depth, ρ_{HI} is the density of atomic hydrogen and $\bar{\rho}_H$ is the mean hydrogen density of the universe (we have used the approximations $\tau \ll 1$ and $\Omega_{m0}(1 + z)^3 \gg 1$). Therefore, the detailed spectrum of the CMB at the long wavelengths of the redshifted 21cm, when observed with high angular resolution, contains precious information on the patchwork of density, spin temperature, and ionization inhomogeneities during the era when the intergalactic medium was still atomic (Hogan & Rees 1979; Scott & Rees 1990; Kumar, Padmanabhan, & Subramanian 1995; Madau, Meiksin, & Rees 1997; Shaver et al 1999; Tozzi et al. 2000; Iliev et al. 2002).

The hydrogen spin temperature plays a key role in determining the amplitude of the 21cm emission or absorption signal against the CMB. At the same time, the evolution of the spin temperature depends on the gas kinetic temperature, and the way that the hyperfine

structure level populations couple to the CMB and the kinetic temperatures. The adiabatic cooling of the hydrogen due to the expansion of the universe causes the gas temperature to decline as $(1+z)^2$, while the CMB temperature is decreasing only as $1+z$, so the gas cools below the CMB. At redshifts $z \gtrsim 100$, the residual ionization left over from the epoch of recombination (Peebles 1968) keeps the gas kinetic temperature at the CMB temperature owing to the heating produced by electron scattering of the CMB, but below this redshift this heating source becomes small and the gas temperature drops below the CMB. If the spin temperature can be coupled to the kinetic temperature at this stage, the atomic medium would be observed in absorption.

The coupling of the spin and kinetic temperatures can be achieved by atomic collisions or by scattering of Ly α photons. The coupling due to atomic collisions is small except at very high redshift, where observations of the redshifted 21cm radiation becomes more difficult, or for unrealistically high values of Ω_b (Scott & Rees 1990). A stronger coupling can be induced by Ly α photons, which should be produced as soon as the first stars are formed. The Ly α photons couple the spin and kinetic temperatures by being repeatedly scattered in the gas. The resonance scattering of a photon consists of a transition from $n = 1$ to $n = 2$, followed by the opposite downward transition. This scattering process can change the population of the hyperfine structure levels (Wouthuysen 1952; Field 1958). The probabilities for a transition back to the ground or excited hyperfine structure states depend on the slope of the radiation spectrum near the Ly α line center, or the “color temperature”. When the radiation spectrum reaches a steady state, this color temperature near the Ly α line center is equal to the gas kinetic temperature, so the Ly α scatterings introduce a thermal coupling between the spin and kinetic temperature. The result of these couplings is that the spin temperature is given by (Field 1958, 1959)

$$T_S = \frac{T_{CMB} + y_\alpha T_k + y_c T_k}{1 + y_\alpha + y_c}, \quad (2)$$

where

$$y_\alpha \equiv \frac{P_{10} T_*}{A_{10} T_k}; \quad y_c \equiv \frac{C_{10} T_*}{A_{10} T_k}. \quad (3)$$

Here, T_k is the kinetic temperature, $T_* = 0.0682\text{K}$ is the hyperfine energy splitting, $A_{10} = 2.87 \times 10^{-15} \text{s}^{-1}$ is the spontaneous emission coefficient of the 21cm line, and $C_{10} = \kappa_{10} n_H$ is the collisional de-excitation rate of the excited hyperfine level. The value of κ_{10} ranges from 2×10^{-14} to $2.5 \times 10^{-10} \text{cm}^3 \text{s}^{-1}$ for T in the range 1 – 1000 K and was tabulated in Allison & Dalgarno (1969).

The indirect de-excitation rate P_{10} of the hyperfine structure levels is related to the total Ly α scattering rate P_α by $P_{10} = 4P_\alpha/27$ (Field 1958), which is given by $P_\alpha = \int d\nu c n_\nu \sigma(\nu)$,

where n_ν is the number density of photons per unit frequency, and $\sigma(\nu)$ is the cross section for Ly α scattering (Madau, Meiksin, & Rees 1997, hereafter MMR).

Besides coupling the spin temperature and kinetic temperature of the gas, the scattering of Ly α photons may also heat up the gas. In this paper, we present the scattering rate and heating rate due to Ly α photons in a uniform atomic intergalactic medium as a function of the two parameters they depend on: the gas temperature and the Ly α scattering optical depth of the medium (or Gunn-Peterson optical depth).

There are two different ways in which photons propagating through the atomic medium may reach the Ly α line, and start being repeatedly scattered by hydrogen: (a) Photons that are emitted between the Ly α and Ly β wavelengths by sources such as massive stars will be redshifted as they penetrate the atomic medium until they reach the Ly α wavelength. These photons enter the Ly α line from its blue wing, and will be called *continuum* photons in this paper. (b) Photons that are emitted at wavelengths shorter than Ly β , but still longer than the Lyman limit so that they can penetrate deep into the atomic medium, will redshift until they reach the Ly β or a higher Lyman series line, and will then be converted into a Ly α photon when the hydrogen atom they excite decays first to the 2p state before reaching the ground state. These photons will be injected near the Ly α line center with a distribution determined by the Voigt function, and will be called *injected* photons. These two types of photons result in different scattering and heating rates, so results will be presented separately for both of them.

MMR estimated the heating rate due to Ly α photons by assuming that the average relative change in a Ly α photon energy in each scattering is the same as when the photon is scattered by an atom at rest: $\langle \Delta E/E \rangle = -h\nu_\alpha/m_H c^2$. Hence, they assumed that the total energy transfer rate is

$$\dot{E} = -\langle \frac{\Delta E}{E} \rangle h\nu_\alpha P_\alpha. \quad (4)$$

At the thermalization rate $P_{th} = 27A_{10}T_{CMB}/4T_*$ (which is the rate P_α required to bring the spin temperature close to the kinetic temperature), the heating rate assumed by MMR is $\dot{E}/k_B \simeq 220 \text{ K Gyr}^{-1}(1+z)/7$, which would heat up the gas kinetic temperature above the CMB temperature in a fraction of a Hubble time at $z \sim 6$.

In the present investigation we calculate the heating rate of the continuum and injected Ly α photons by computing the background spectrum near the Ly α line using the Fokker-Planck method introduced by Rybicki & Dell'antonio (1994) (hereafter RD), and using energy conservation. We find that the heating rate due to Ly α scattering is much smaller than the estimate of eq. (4), and as a consequence Ly α photons do not constitute a significant heating source of the gas. Calculating the heating rate caused by Ly α photons as

if every atom were at rest, without taking into account the thermal motions, is incorrect, and as we shall see the heating rate per unit volume is not proportional to the atomic density. We explain in the Appendix the reason why the argument used by MMR in their Appendix B to justify using eq. (4) for the heating rate is invalid. As pointed out by MMR, X-rays are important in pre-heating the atomic medium before it is reionized. In fact, our work leads to the conclusion that X-rays are the only important source of heating before the atomic medium is reached by an ionization front.

This paper is organized as follows: in §2 we describe our method of calculation. We present our result on scattering and heating rates in §3, explaining the physical reason why gas is not heated by Ly α photons as if every atom were at rest. We illustrate the consequences for future 21cm observations in §4, with an example for the evolution of the spin temperature with redshift, including also a model for X-ray heating. Our conclusions are summarized in §5. We adopt a flat Λ CDM model with the following cosmological parameters: $h_0 = 0.7$, $\Omega_\Lambda = 0.7$, $\Omega_m = 0.3$, $\Omega_b h_0^2 = 0.021$, $Y_{\text{He}} = 0.24$.

The code for solving the line profile and calculating the scattering and heating rates is available from the authors¹.

2. Method of Calculation

Our goal in this work is to compute the Ly α scattering rate and the heating rate of hydrogen induced by this scattering, from which one can then compute the evolution of the spin temperature. The scattering and heating rates can be calculated once the background spectrum near the Ly α line is known. Let us consider the background of photons produced by constant, flat spectrum sources in an expanding universe (in practice the intrinsic source spectrum does not matter because Ly α scattering is important only on a very narrow range of frequencies around Ly α , in which the intrinsic source spectrum can be considered to be constant). In the absence of scattering, the photons would simply redshift and would produce a photon number density per unit frequency $n(\nu) = n_0$ that is independent of frequency near Ly α . The presence of scatterings by hydrogen introduces a feature in the spectrum around the Ly α line, which has a constant shape $n(\nu)$ once a steady-state is reached. Given this spectrum, the rate at which Ly α photons are being scattered is given by the integral

$$P_\alpha = c \int d\nu n(\nu) \sigma(\nu) . \quad (5)$$

¹Our code, named “Lyman Alpha scattering and Spin Temperature”, or LAST, can be downloaded at <http://theory.kitp.ucsb.edu/~xuelei/LAST>.

Here, $\sigma(\nu)$ is the Ly α scattering cross section as a function of frequency. The cross section has a thermal width $\Delta\nu_D$ determined by the temperature T of hydrogen atoms of mass m_H ,

$$\Delta\nu_D = \frac{\sqrt{2k_B T/m_H}}{c} \nu_\alpha , \quad (6)$$

where ν_α is the Ly α line central frequency and k_B is the Boltzmann constant. The cross section at the line center is

$$\sigma_0 = \frac{\pi e^2}{m_e c} f_{12} [\Delta\nu_D]^{-1} , \quad (7)$$

where $f_{12} = 0.416$ is the oscillator strength for the Ly α transition. The dependence of the cross section on frequency is given by the normalized Voigt function,

$$\phi(x) = \frac{a}{\pi^{3/2}} \int_{-\infty}^{\infty} dy \frac{e^{-y^2}}{(x-y)^2 + a^2} , \quad (8)$$

where $x = (\nu - \nu_\alpha)/\Delta\nu_D$, the Voigt parameter is $a = A_{21}/(8\pi\Delta\nu_D)$, and $A_{21} = 6.25 \times 10^8$ Hz is the Einstein spontaneous emission coefficient. We will also use the photon intensity $J(\nu) = c n(\nu)/(4\pi)$. With these definitions, the scattering rate is

$$P_\alpha = 4\pi\sigma_0 \Delta\nu_D \int J(x)\phi(x)dx . \quad (9)$$

The heating rate of the gas induced by Ly α scattering can be simply obtained by requiring conservation of energy. The scatterings cause the cosmic background to have a narrow spectral feature around the Ly α wavelength. Were the scatterings to cease at a certain instant, this feature would simply be redshifted to longer wavelengths. Instead, when a steady-state spectrum is reached, the feature is fixed at a constant wavelength. The reduction in energy per unit volume of the background due to this feature is $\Delta\epsilon = \int d\nu [n_0 - n(\nu)] h\nu d\nu$ (for the purpose of this discussion we ignore the photons injected at the Ly α wavelength by recombinations, so that in the absence of scatterings, $n(\nu) = n_0$; injected photons will be fully considered later). Over an interval of time dt , the energy per unit volume that the background photons must lose to keep the spectral feature at a fixed wavelength is $\Delta\epsilon(d\nu/\nu) = \Delta\epsilon H dt$, where $d\nu$ is the change in frequency due to redshift over the interval dt , and H is the Hubble constant at time t . The energy lost by the photons must be gained by the hydrogen atoms, so the gas heating rate per unit volume is

$$\Gamma = H\Delta\epsilon = H \int [n_0 - n(\nu)] h\nu d\nu = \frac{4\pi H h \Delta\nu_D}{c} \int [J_0 - J(\nu)] \nu d\nu . \quad (10)$$

We use these equations in §3 to compute the scattering and heating rates once the line spectrum has been calculated. An alternative derivation of the heating rate in equation (10) is given in the Appendix.

The spectrum of the cosmic background near Ly α is determined by the radiative transfer equation for resonant scattering for a homogeneous and isotropic expanding universe, which is (RD)

$$\frac{\partial J(x, \tau)}{\partial \tau} = -\phi(x)J(x, \tau) + \gamma_S \frac{\partial J(x, \tau)}{\partial x} + \int R_{II}(x, x')J(x', \tau)dx' + C(\tau)\psi(x), \quad (11)$$

where $\tau = (cn_1\sigma_0)t$ is the mean free time between scatterings for a photon at the line center, t is the physical time, and $n_1 \simeq n_H$ is the number density of hydrogen atoms in the ground state. The Sobolev parameter is $\gamma_S = \tau_{GP}^{-1}$, where $\tau_{GP} = (\pi e^2 n_1 f_{12})/(H m_e \nu_\alpha)$ is the Gunn-Peterson optical depth. The first term in the right-hand-side of equation (11) describes the removal of photons that are scattered, and the second term accounts for the redshift. The third term represents the addition of the photons redistributed over frequency after scattering (Rybicki & Hummer 1992), and the fourth term is due to the injection of new Ly α photons with a spectral profile $\psi(x)$.

In the Fokker-Planck approximation, the scattering problem is treated as diffusion in the approximation that the width of the spectral feature is large compared to the frequency change in typical scatterings. The redistribution term then becomes (RD)

$$\int R_{II}(x, x')J(x', t)dx' = \phi(x)J(x) + \frac{1}{2} \frac{\partial}{\partial x} \left[\phi(x) \frac{\partial J(x)}{\partial x} + 2\eta\phi(x)J(x) \right], \quad (12)$$

where the recoil term is included, with $\eta = h\nu_\alpha/(c\sqrt{2m_H k_B T})$. This approximation conserves photon number. The equation is then reduced to [see eq. (34) of RD]

$$\frac{\partial J}{\partial \tau} = \frac{1}{2} \frac{\partial}{\partial x} \left[\phi \frac{\partial J}{\partial x} + 2\eta\phi J \right] + \gamma_S \frac{\partial J}{\partial x} + C(t)\psi(x). \quad (13)$$

When the equilibrium state is reached, $\partial J/\partial \tau = 0$.

Since this equation is linear, we can write its solution as $J = J_c + J_i$, where J_c is the spectrum of the continuum photons, and J_i is the spectrum of the recombination photons injected near the line center.

For the continuum photons, there is no injection and so $C(t) = 0$. Equation (13) is reduced to

$$\phi(x) \frac{d}{dx} J_c(x) + 2 [\eta\phi(x) + \gamma_S] J_c(x) = A, \quad (14)$$

where A is a constant of integration determined by the boundary condition: as $x \rightarrow \infty$, $\phi(x) \rightarrow 0$, $J_c \rightarrow J_{c0}$, where $J_{c0} = (4\pi/c) n_{c0}$ is the unperturbed intensity. Therefore, $A = 2\gamma_S J_0$. The equation is then solved as an initial value problem of an ordinary differential equation with the condition $J_c(x) \rightarrow J_{c0}$ for $x \rightarrow -\infty$, required by photon number conservation.

In Fig. 1, we plot the solution for a typical case: $T = 2.65\text{K}$ and $\gamma_S = 1.44 \times 10^{-6}$, corresponding to the physical conditions of unheated gas at $z = 10$ in a flat ΛCDM model. An absorption feature is produced near the center of the line.

For the injected photons, we assume a constant source $C(t) = C$. This should generally be an accurate approximation because the timescale for the evolution of the production rate of Ly α photons from sources is likely be of order the Hubble time, which is much longer than the relaxation time, which is of order the time to redshift across the width of the Ly α spectral profile of the cosmic background. We also inject photons with a single frequency at the Ly α line center, i.e., $\psi(x) = \delta(x)$. Because photons change randomly in frequency over a thermal width at each scattering, and the number of scatterings each photon undergoes is very large, injecting the photons with a thermal width instead does not make any difference to the final profile [we have verified this by obtaining solutions with $\psi(x)$ given by a Voigt profile, which did not result in any significant change to the resulting spectral profile]. The solution is

$$\phi(x) \frac{d}{dx} J_i(x) + 2 [\eta\phi(x) + \gamma_S] J_i(x) = -2C\Theta(x) + B, \quad (15)$$

where $\Theta(x)$ is the Heaviside step function. The value of the integration constant B can again be determined from boundary conditions: as $x \rightarrow +\infty$, we must now have $J_i(x) \rightarrow 0$, from which we obtain $B = 2C$. The profile of the line can again be obtained by solving eq. (15), with the initial condition $J_i(x = -\infty) = J_{i0}$, where J_{i0} is the photon intensity due to the injected photons. The result is shown in Fig. 2, for two different temperatures; we see that some of the photons injected at the line center are scattered to the right (blue) side.

We note that the solution for the spectral profile of continuum and injected photons has a characteristic width in the variable $x = \nu/\Delta\nu_D$ that is substantially larger than unity, implying that the Fokker-Planck approximation we have used should be accurate.

3. Results

The heating and scattering rates are of course proportional to the background intensity. During the epoch of reionization, at least one ionizing photon has to be emitted for every baryon in the universe, and more if the typical baryon can recombine many times. The number of Ly α photons emitted is of the same order for sources without a large Lyman break, and can be much larger if many ionizing photons are internally absorbed. We use the intensity corresponding to one photon per hydrogen atom in the universe as a fiducial value:

$$\tilde{J}_0(z) = \frac{n_H c}{4\pi\nu_\alpha} = 1.65 \times 10^{-13} (1+z)^3 \left(\frac{\Omega_b h_0^2}{0.02} \right) \text{ cm}^{-2}\text{s}^{-1}\text{sr}^{-1}\text{Hz}^{-1}, \quad (16)$$

where n_H is the hydrogen number density. For reference to other work, we quote also the value of the energy intensity of this unit: $\tilde{J}_0 h\nu_\alpha = 2.69 \times 10^{-24} (1+z)^3 (\Omega_b h_0^2 / 0.02) \text{ erg cm}^{-2} \text{ s}^{-1} \text{ sr}^{-1} \text{ Hz}^{-1}$. The heating rate in equation (10) can be reexpressed as a heating rate per hydrogen atom and per Hubble time. For the continuum photons, it is:

$$\frac{\Gamma_c}{Hn_H k_B} = \frac{h\Delta\nu_D}{k_B} \frac{J_{c0}}{\tilde{J}_0} \int dx \left[1 - \frac{J_c(x)}{J_{c0}} \right] \equiv \sqrt{2T T_0} \frac{J_{c0}}{\tilde{J}_0} I_c , \quad (17)$$

where we have defined $I_c = \int dx [1 - J_c(x)/J_{c0}]$, and $T_0 = (h\nu_\alpha)^2 / (k_B m_H c^2) = 1.29 \times 10^{-3}$ K. For the example shown in Figure 1, the integral is the shaded area, $I_c = 16.7$. It is clear from equation (17) that if the number of photons in the background is not greater than one per hydrogen atom, the heating rate due to Ly α scattering is not very large because $T_0 \ll T$. In the example of $T = 2.65$ K at $z = 10$, equation (17) yields $\Gamma_c / (Hn_H k_B) = 1.4$ K (J_{c0} / \tilde{J}_0).

Similarly, for the injected photons with a δ -function profile, the heating rate is

$$\frac{\Gamma_i}{Hn_H k_B} = \frac{h\Delta\nu_D}{k_B} \frac{J_{i0}}{\tilde{J}_0} \left\{ \int_{-\infty}^0 dx \left[1 - \frac{J_i(x)}{J_{i0}} \right] - \int_0^{+\infty} dx \frac{J_i(x)}{J_{i0}} \right\} \equiv \sqrt{2T T_0} \frac{J_{i0}}{\tilde{J}_0} I_i . \quad (18)$$

We note that, for the more exact case in which photons are injected with a Voigt profile in frequency, the heating rate is obtained by subtracting from $J_i(x)$ the steady-state solution of the background with no scattering (shown in Fig. 3 of RD). However, one can easily prove that the result is exactly the same as what is obtained by subtracting instead the step function spectrum that results from a δ function of the injected photons.

In Fig. 2, we show the spectrum J_i for two different temperatures: $T_k = 2.65$ K and $T = 1$ K, for $\gamma_S = 1.44 \times 10^{-6}$. In the $T_k = 2.65$ K case, we have $\Gamma_i / (Hn_H k_B) = -0.104$ K (J_{i0} / \tilde{J}_0). This negative heating rate means that the scattering of these injected photons actually cools the gas, because some of the photons are scattered to the blue side of the spectrum and gain energy from the hydrogen gas. At lower gas temperatures, as in the $T_k = 1$ K case shown in the figure, $\Gamma_i / (Hn_H k_B) = 0.40$ K (J_{i0} / \tilde{J}_0), the photons heat the gas. However, at $z = 10$ the temperature of adiabatically expanding gas is 2.65 K, and there is no known mechanism which could cool the gas below this temperature, so the net effect of the injected photons must be to cool the gas. In any case, both the heating rate due to continuum photons and the cooling rate due to injected photons are very small.

To calculate the spin temperature from equation (2), we also need to know the scattering rate of the Ly α photons in equation (9), which can be reexpressed as

$$P_\alpha = H\tau_{GP} \int \frac{J(x)}{\tilde{J}_0} \phi(x) dx . \quad (19)$$

We define

$$S_c \equiv \int \frac{J_c(x)}{J_{c0}} \phi(x) dx, \quad S_i \equiv \int \frac{J_i(x)}{J_{i0}} \phi(x) dx . \quad (20)$$

We plot the integrals I_c , I_i , S_c , and S_i as a function of $\gamma_S = \tau_{GP}^{-1}$, for several different temperatures, in Figures 3- 4. Our code calculates the values of these integrals for any given gas temperature and optical depth.

The intensity corresponding to the thermalization rate required to bring the spin temperature down to the kinetic temperature (see the introduction) is

$$\frac{J_0}{\bar{J}_0} = \frac{P_\alpha}{H\tau_{GPS}} = \frac{27A_{10}T_{CMB}\gamma_S}{4T_* HS}, \quad (21)$$

where the subscripts c or i can be applied. For the case $\gamma_S = 1.44 \times 10^{-6}$ and $T = 2.65$ K at $z = 10$, S_i or S_c are close to one and we find $J_0/\bar{J}_0 \simeq 0.3$. Thus, from our earlier result that the heating rate in this case is $\Gamma_c/(Hn_H k_B) = 1.4$ K (J_{c0}/\bar{J}_0) for the case of continuum photons, we find that over the time that continuum Ly α photons bring the spin temperature down to the gas temperature, they should heat the gas by only ~ 0.5 K, and injected photons should cool the gas by ~ 0.03 K.

The reason why the heating rate is much less than the value obtained by assuming that each atom loses the same average energy at each scattering as if it were at rest is that the intensity of the background spectrum drops steeply at the Ly α line center, as shown in Figures 1 and 2. The vast majority of the scatterings occur within a few thermal widths of the line center, where the color temperature of the spectrum (reflecting its slope) is almost equal to the kinetic temperature. When these two temperatures are the same, there obviously cannot be any heat exchange between photons and atoms because they are in thermodynamic equilibrium. The heating from continuum photons occurs because the color temperature is slightly larger than the kinetic temperature. Injected photons have a temperature slightly lower than the kinetic temperature, so they cool the gas. Cooling is caused by photons that are on the red side of the line center because these photons are more likely to be scattered by atoms moving in the direction opposite to the photon (for which the Doppler effect can shift the photon frequency to the line center), and these atoms will be slowed down by the scattering. When the color temperature is below the kinetic temperature, the cooling effect due to the preferential scattering of photons moving in the opposite direction than the atoms is greater than the heating effect due to recoil from photons moving in a random direction.

The heating or cooling rates per unit volume are not proportional to the atom density. If the atom density is increased, not only the number of scatterings increases, but also the color temperature is brought closer to the kinetic temperature because of the increased rate of interaction between atoms and photons, and the average energy exchanged between them at each scattering is reduced. The heating rate changes only with the width of the background spectral feature that determines the integrals I_c and I_i , according to the energy conservation argument used in §2.

In the calculation of the spin temperature evolution from equation (2), we assume that the color temperature of the Ly α photons is equal to the gas kinetic temperature. This is true at the line center in the limit of large optical depth (Field 1958, 1959), but the slope of the photon distribution varies outside the line center. In the more general case, equations (2)-(3) can be generalized as

$$y_\alpha T_k \rightarrow \int dx y_\alpha(x) T_\alpha(x) = \frac{T_*}{A_{10}} \frac{4}{27} \int dP_\alpha(x) \quad (22)$$

$$y_\alpha \rightarrow \int dx y_\alpha(x) = \frac{T_*}{A_{10}} \frac{4}{27} \int dP_\alpha(x) / T_\alpha(x) \quad (23)$$

where the color temperature T_α at x is defined by

$$\frac{J'(x)}{J(x)} \equiv -\frac{h\nu}{k_B T_\alpha(x)} \approx -\frac{h\nu_0}{k_B T_\alpha(x)}, \quad (24)$$

and

$$dP_\alpha(x) = 4\pi\sigma_0 \Delta\nu_D J(x) \phi(x) dx \quad (25)$$

Because the vast majority of scatterings occur near the line center, where the color temperature and kinetic temperature are very nearly the same, this generalization does not significantly change the result for the spin temperature. We have found by a numerical test that this correction affects the spin temperature by only a small fraction of a percent.

4. Simple Models for the Thermal Evolution

We will now consider a simple model where the emissivity of Ly α photons turns on at a redshift z_i and increases linearly with redshift thereafter. We will also consider the effect of X-ray emission from the same star formation regions, which dominates the heating rate of the gas. This will illustrate a plausible thermal history of the gas and the expected strength of the absorption or emission signal in the redshifted 21cm line.

The kinetic temperature of the gas in the expanding Universe evolves as

$$(1+z) \frac{dT_k}{dz} = 2T_k - \frac{2}{3} \frac{(\Gamma_{tot} - \Lambda_{tot})}{(Hn k_B)}, \quad (26)$$

where Γ_{tot} and Λ_{tot} are the total heating and cooling rates, respectively, and n is the total gas number density.

In the absence of heating and cooling, the gas temperature decreases adiabatically with $T \propto (1+z)^2$. We use the code RECFAST ² (Seager, Sasselov, & Scott 1999; Seager,

²<http://www-cfa.harvard.edu/~sasselov/rec>

Sasselov & Scott 2000) to calculate the temperature evolution of the gas before the first stars and quasars turn on. We note that at $z \gtrsim 40$ the spin temperature drops below the CMB temperature due to the collisional coupling (in Fig. 6, this drop is seen at the highest redshift end). The corresponding absorption is, however, difficult to observe at the very long wavelengths corresponding to this redshift. At lower redshifts, the spin temperature is practically equal to the CMB temperature until the first Ly α photons are produced.

4.1. Ly α emissivity

If the comoving photon emissivity (defined as the number of photons emitted per unit comoving volume, time and frequency) at the Ly α line from stars at redshift z is $\epsilon(\nu_\alpha, z)$, then the *comoving* Ly α photon intensity at redshift z is given by

$$J_{c0}(z) = \frac{1}{4\pi} (1+z)^{\alpha_S} \int_z^{z_{max}} \frac{c}{H(z')} \epsilon(\nu_\alpha, z') (1+z')^{-(1+\alpha_S)} dz', \quad (27)$$

where the emissivity spectrum is assumed to be $\epsilon(\nu) \propto \nu^{-\alpha_S-1}$, and z_{max} is determined by the condition that only the photons emitted at frequencies lower than the Ly β line will not interact with the intergalactic medium:

$$(1+z_{max}) = \frac{\nu_\beta}{\nu_\alpha} (1+z) = \frac{32}{27} (1+z) \quad (28)$$

To discuss the plausible range of values of the comoving emissivity, it is convenient to introduce the unit

$$\tilde{\epsilon} \equiv \frac{n_H H}{\nu_\alpha} = \frac{4\pi}{c} H \tilde{J}_0. \quad (29)$$

Thus, if $\epsilon = \tilde{\epsilon}$, one photon is being emitted per hydrogen atom and per Hubble time, per unit $\log(\nu)$.

During the epoch of reionization, at least one photon must be emitted for every baryon in the universe. For a homogeneous medium, the recombination rate αn_e^2 is equal to the Hubble rate, H , at $z \simeq 6$; hence, if reionization takes place during the interval $20 \gtrsim z \gtrsim 6$, a few photons should be emitted for every baryon to ionize them and to compensate for recombination. The number of recombinations can be increased due to the clumping factor of the ionized intergalactic gas (see, however, Miralda-Escudé, Haehnelt & Rees 2000 for a discussion of why the clumping factor of ionized gas is probably not much larger than unity during the epoch of reionization). If these ionizing photons are produced by star-forming regions, then the photon emissivity per unit $\log(\nu)$ between Ly α and the Lyman limit should be 3 to 5 times larger than the emissivity of ionizing photons, owing to the average Lyman

break of the atmospheres of massive stars with a Salpeter Initial Mass Function (e.g., Bruzual & Charlot 1993). The photons between Ly α and the Lyman limit may have a larger escape fraction from the star formation regions than the ionizing photons (if some of the absorption is due to local hydrogen with low dust content), in which case the ratio of the emissivity between Ly α and Lyman limit to the ionizing emissivity would be further increased. This suggests that the emissivity near Ly α should be at least $\epsilon \gtrsim 10\tilde{\epsilon}$.

The total number of ionizing photons emitted is also related to the metallicity produced by massive stars. To produce one ionizing photon per baryon, the mean metallicity of the universe must be raised by 10^{-5} , or $5 \times 10^{-4} Z_{\odot}$ (e.g., Madau & Shull 1996). If the typical metallicity in the Ly α forest and damped Ly α systems at $z \gtrsim 3$, which is $Z \sim 10^{-2} Z_{\odot}$, is not to be exceeded, one cannot produce more than ~ 20 ionizing photons per baryon, implying that $\epsilon \lesssim 100\tilde{\epsilon}$ at Ly α .

As a simple model of the Ly α background evolution, we assume that the Ly α emissivity increases linearly from 0 at some initial redshift z_i ,

$$\epsilon(z) = \begin{cases} 0; & z > z_i \\ \epsilon_r \frac{z_i - z}{z_i - z_r}; & z_r < z < z_i \end{cases} \quad (30)$$

We will use two values for the peak emissivity at Ly α , ϵ_r , reached at z_r : $\epsilon_r = 10\tilde{\epsilon}$ and $\epsilon_r = 100\tilde{\epsilon}$, based on the previous discussion. Assuming also a flat spectrum, $\alpha_S = 0$, the Ly α intensity due to the continuum photons is then

$$\frac{J_{c0}(z)}{\tilde{J}_0} = \frac{\epsilon_r}{\tilde{\epsilon}} g(1+z), \quad (31)$$

where the function g is

$$g(x) = \frac{x^{3/2}}{z_i - z_r} \left[\frac{2}{3}(1+z_i) \left(x^{-3/2} - x_{<}^{-3/2} \right) - 2 \left(x^{-1/2} - x_{<}^{-1/2} \right) \right], \quad z < z_i \quad (32)$$

and

$$x_{<} = \min \left[(1+z_i), \left(\frac{32}{27}x - 1 \right) \right]. \quad (33)$$

The resulting proper Ly α intensity is plotted as the function $(1+z)^3 J_{c0}/\tilde{J}_0$ in Fig. 5, for $z_r = 6$ and $\epsilon_r/\tilde{\epsilon} = 10$, for two cases of initial redshift: $z_i = 20$ and $z_i = 12$. The proper Ly α intensity increases rapidly after z_i and then decreases as z decreases due to the $(1+z)^3$ factor.

We will assume that $J_{i0} = J_{c0}$. The injected photons have a comparable intensity to the continuum ones, because the photons emitted between Ly β and the Lyman limit are similar

to those emitted between Ly α and Ly β , and a large fraction of the Lyman continuum photons will eventually result in an injected Ly α photon when the atom that they ionize recombines again.

4.2. Heating by soft X-rays

Since the scattering of Ly α photons produces a negligible heating rate for the gas, the main heating mechanism should be soft X-ray photons. The soft X-rays can be emitted by a number of sources associated with star-forming regions, such as X-ray binaries, supernova remnants and QSOs.

X-ray photons have a photoionization cross section that is much smaller than that of the ionizing photons near the hydrogen ionization potential, so they can penetrate deep into the neutral regions of the intergalactic medium. There, they photoionize hydrogen or helium, and the high-energy electron that is produced can then transfer a fraction of its energy to the gas by Coulomb collisions with other electrons and protons. Once the energy has been thermalized among the charged particles at a temperature low enough to avoid losses by collisional excitation of hydrogen, the thermal energy can be transferred to the hydrogen atoms in slow collisions involving dipole interaction. The fraction of the X-ray energy that can be converted to the gas thermal energy (rather than being used in collisional ionizations and excitations of hydrogen or helium) depends on the fractional ionization of the gas. Using the RECFAST code, we found that the initial ionized fraction from the recombination era (before more ionizations are caused by the X-rays) is 2×10^{-4} , which implies that a fraction of 14% of the X-ray energy is used to heat the gas (Shull & Van Steenberg 1985). As the fraction of free electrons increases, this fraction also increases, but for simplicity we shall assume it a constant.

We parameterize the emissivity in X-rays in terms of the fraction of the energy that is emitted in X-rays compared to the energy emitted at Ly α per unit $\log \nu$, which we designate as α_x . The X-ray heating rate is then

$$\Gamma_x(z) = 1.4 \times 10^{-3} \left(\frac{\alpha_x}{0.01} \right) h \epsilon(z) , \quad (34)$$

where $\epsilon(z)$ is given in Eq. (30), and h is the Planck constant. At $z = 6$, the heating rate due to X-rays in this model is

$$\frac{\Gamma_x}{n_H H k_B} = 1.7 \times 10^3 \left(\frac{\alpha_x}{0.01} \right) \frac{\epsilon_r}{10 \tilde{\epsilon}} \text{ K} . \quad (35)$$

Therefore, by emitting only $\sim 1\%$ of the energy as X-rays, the sources can rapidly heat the intergalactic medium to temperatures above the CMB.

4.3. Results for thermal evolution and the 21 cm Antenna Temperature

The evolution of the gas kinetic and spin temperatures in the absence of X-ray heating is plotted in Fig. 6, for two values of the initial redshift ($z_i = 20$ and $z_i = 12$), and two values of the emissivity ($\epsilon_r/\tilde{\epsilon} = 10$ and 100).

In the absence of X-rays, the heating due to Ly α scattering is very low and the kinetic temperature of the gas deviates only slightly from the adiabatic curve at late times. For our assumed emissivity of 10 to 100 photons per baryon per Hubble time, the spin temperature drops to values very close to the kinetic temperature, producing a large absorption signal on the CMB of up to 200 mK, as seen in Figure 7.

Figure 8 shows the thermal evolution and the resulting antenna temperature when we include X-ray heating with $\alpha_x = 0.01$, for the case $z_i = 12$ and $\epsilon_r/\tilde{\epsilon} = 10$. With only 1% of the energy emitted as X-rays, the kinetic temperature of the gas increases rapidly when the first sources turn on, leaving only a brief period of absorption in the beginning of small amplitude, which then turns to emission, with an amplitude of less than 20 mK.

5. Conclusion

We have calculated the Ly α photon scattering and heating rates in the atomic intergalactic medium, including both redshifted continuum photons emitted between Ly α and Ly β , and injected photons produced by recombinations or excitations by Ly β and higher Lyman series photons. The heating rate of the gas due to the scattering of these Ly α photons is very small and essentially negligible. In the absence of other heating sources, the gas would continue to cool down almost adiabatically while the spin temperature would rapidly drop to nearly the kinetic temperature given a reasonable emission of photons during the reionization epoch. This would produce a 21cm absorption against the CMB as large as ~ 200 mK, at the average hydrogen density of the universe.

Of course, if the absorption signal can be observed at high angular and frequency resolution, the antenna temperature should fluctuate around its mean value owing to density fluctuations, as well as spin temperature fluctuations that would be produced by spatial variations in the history of the photon emissivity between Ly α and the Lyman limit (e.g. Tozzi et al. 2000; Ciardi & Madau 2003). At the same time, during the epoch of reionization, there should be a gradual increase of the fraction of the volume that is ionized (e.g., Miralda-Escudé 2003), and the average antenna temperature should then be multiplied by the fraction of baryons that remain in atomic form. Because this fraction of baryons should decrease gradually, any 21cm absorption or emission should also vary smoothly with redshift.

Unfortunately, the large absorption signal predicted in the absence of X-ray heating is unlikely to be present. It is very likely that significant X-ray emission is produced within only a few million years of the formation of the first stars in the universe: some of the stars may be in binaries which will evolve into high-mass X-ray binaries, and supernova explosions can also emit soft X-rays (see e.g. Oh 2001; Venkatesan, Giroux, & Shull 2001). Photons with energies as low as 0.2 keV can propagate as far as 3 comoving Mpc over the atomic intergalactic medium at $z \sim 10$ before they are absorbed by hydrogen or helium.

There may still be some ways in which certain regions of the intergalactic medium may be illuminated by Ly α photons from the first stars, without receiving soft X-rays as well. For example, if stars form in a region with a high column density of hydrogen and helium with very little dust, and the hydrogen and/or helium is not fully ionized for a long time, the photons between Ly α and the Lyman limit from stars would escape, while the ionizing and soft X-ray photons might all be locally absorbed. In particular, there is the possibility that singly ionized helium remains self-shielded as massive stars ionize the gas around them. We note from Figure 6 that the time required to bring down the spin temperature can be very short (10^8 years or less) for typical values of the Ly α background intensity, and it is possible that a complete absorption of soft X-rays from the first star-forming regions would persist long enough to allow for a strong 21cm absorption signal in local regions of the intergalactic medium, when they are illuminated by the first light from stars forming in their vicinity. Nevertheless, it seems likely that any decrease of the spin temperature will be short-lived, and that X-ray heating will cause the 21cm signal to switch to emission a short time after the first stars are formed.

Future observations of the 21cm signal in absorption and emission at high angular and frequency resolution have an enormous potential for revealing the details of the reionization epoch. Fluctuations in the antenna temperature arise from both gas density and spin temperature variations. The density fluctuations will inform us of the state of gravitational evolution of primordial fluctuations at the highest attainable redshifts after recombination, while the spin temperature fluctuations will reveal the spatial distribution of the first sources of ultraviolet and X-ray emission in the universe.

This work was supported in part by NSF grants NSF-0098515 and PHY99-07949.

Appendix

MMR assumed that the heating rate per unit volume of the hydrogen gas due to Ly α scattering is equal to the recoil energy given to a hydrogen atom at rest, $(h\nu_\alpha)^2/(m_H c^2)$,

times the scattering rate:

$$\Gamma_{MMR} = \frac{(h\nu_\alpha)^2}{m_H c^2} n_H P_\alpha = \frac{(h\nu_\alpha)^2}{m_H c^2} 4\pi n_H \sigma_0 \Delta\nu_D \int J(x) \phi(x) dx . \quad (1)$$

This heating rate was justified from equation (13) for the time evolution of the photon intensity J . MMR assumed that the rate of heat transfer to the atoms is determined by the change in the spectrum due to the recoil effect, which is the second term in the right-hand-side of equation (13):

$$\left(\frac{\partial J}{\partial \tau} \right)_{recoil} = \frac{\partial(\eta\phi J)}{\partial x} . \quad (2)$$

They then computed the heating rate by integrating the variation in photon energy density per unit physical time over frequency:

$$\Gamma_{MMR} = 4\pi h \Delta\nu_D n_H \sigma_0 \int dx x \frac{\partial(\eta\phi J)}{\partial x} = (H n_H k_B) T_0 \tau_{GP} \frac{J_{c0}}{\tilde{J}_0} S_c , \quad (3)$$

where the integral S_c is given in equation (20), and τ_{GP} is the Gunn-Peterson optical depth (all symbols are defined in §2 and 3; the last equality involves an integration by parts).

However, the first term in equation (13) must also be included to compute the heating rate of the gas. In fact, the heating rate of the gas is not just determined by the recoil, but also by the fact that the background intensity is greater on the red wing of the Ly α line than on the blue wing, and scatterings have an average tendency to bring photons back into the line center. The energy change of the photons due to the first term in equation (13) can only go into the gas (whereas that of the third term is due to redshift and goes into the expansion of the universe, and that of the fourth term is provided by a source). Thus, the correct heating rate is

$$\Gamma = 4\pi h \Delta\nu_D n_H \sigma_0 \int dx x \frac{\partial}{\partial x} \left(\frac{\phi}{2} \frac{\partial J}{\partial x} + \eta\phi J \right) . \quad (4)$$

Under steady-state conditions (and no source term; here, we consider continuum photons only, to simplify the discussion), we can replace the quantity inside parenthesis by $-\tau_{GP}^{-1} \partial J / \partial x$, and integrating by parts, we obtain

$$\Gamma = (H n_H k_B) \sqrt{T_0 T} \frac{J_{c0}}{\tilde{J}_0} I_c , \quad (5)$$

which is the expression in equation (17). Note that, because $\tilde{J}_0 = (n_H c) / (4\pi\nu_\alpha)$, the heating rate per unit volume is independent of the atomic density, except for the weak dependence of I_c on τ_{GP} , whereas MMR assumed that the heating rate *per atom* is independent of n_H .

REFERENCES

Abel, T., Bryan, G. L., & Norman, M. L. 2000, *ApJ*, 540, 39.

Allison, A. C. & Dalgarno, A., 1969, *ApJ*, 158, 423.

Becker, R. H. et al, 2001, *AJ*, 122, 2850

Bromm, V., Coppi, P. S., & Larson, R. B. 2002, *ApJ*, 564, 23.

Bruzual, A., & Charlot, S. 1993, *ApJ*, 405, 538.

Ciardi, B. & Madau, P., submitted to *ApJ*, preprint astro-ph/0303249.

Couchman, H. M. P., & Rees, M. J., 1986, *MNRAS*, 221, 53.

Fan, X., et al, 2002, *AJ*, 123, 1247.

Fan, X., et al, 2003, *AJ*, in press (astro-ph/0301135).

Field, G. B., 1958, *Proc. IRE*, 46, 240.

Field, G. B., 1959, *ApJ*, 129, 551.

Gnedin, N. Y., 2000, *ApJ*, 535, 530.

Gunn, J. E., & Peterson, B. A., 1965, *ApJ*, 142, 1633.

Hogan, C. J. & Rees, M. J., 1979, *MNRAS*, 188, 791.

Iliev, I. T., Shapiro, P. R., Ferrara, A., Martel, H., 2002, *ApJ*, 572, L123.

Kumar, A., Padmanabhan, T., & Subramanian, K., 1995, *MNRAS*, 272, 544.

Madau, P., Meiksin, A., & Rees, M. J., 1997, *ApJ*, 475, 429. (MMR)

Madau, P., & Shull, J. M. 1996, *ApJ*, 457, 551.

Miralda-Escudé, J., 2003, *ApJ*, 597, in press (astro-ph/0211071).

Miralda-Escudé, J., Haehnelt, M., & Rees, M. J. 2000, *ApJ*, 530, 1.

Oh, S. P., 2001, *ApJ*, 553, 499.

Peebles , P. J. E. 1968, *ApJ*, 153, 1.

Rybicki, G. B., & Dell'antonio, I. P., 1994, *ApJ*, 427, 603. (RD)

Rybicki, G. B., & Hummer, D. G., 1992, *ApJ*387, 248.

Scott, D. & Rees, M. J., 1990, *MNRAS*, 247, 510.

Seager, S., Sasselov, D., & Scott, D. 1999, *ApJ*, 523, L1.

Seager, S., Sasselov, D., & Scott, D. 2000, *ApJS*, 128, 407.

Shaver, P. A., Windhorst, R. A., Madau, P., de Bruyn, A. G., 1999, *A&A*, 345, 380.

Shull, J. M., & Van Steenberg, M. E., 1985, *ApJ*, 298, 268.

Tegmark, M., Silk, J., Rees, M. J., Blanchard, A., Abel, T., Palla, F., 1997, *ApJ*, 474, 1.

Tozzi, P., Madau, P. Meiksin, A., & Rees, M. J., 2000, *ApJ*, 528, 597.

Venkatesan, A., Giroux, M. L., Shull, J. M., 2001, *ApJ*, 563, 1.

Wouthuysen, S. A., 1952, *AJ*, 57, 31.

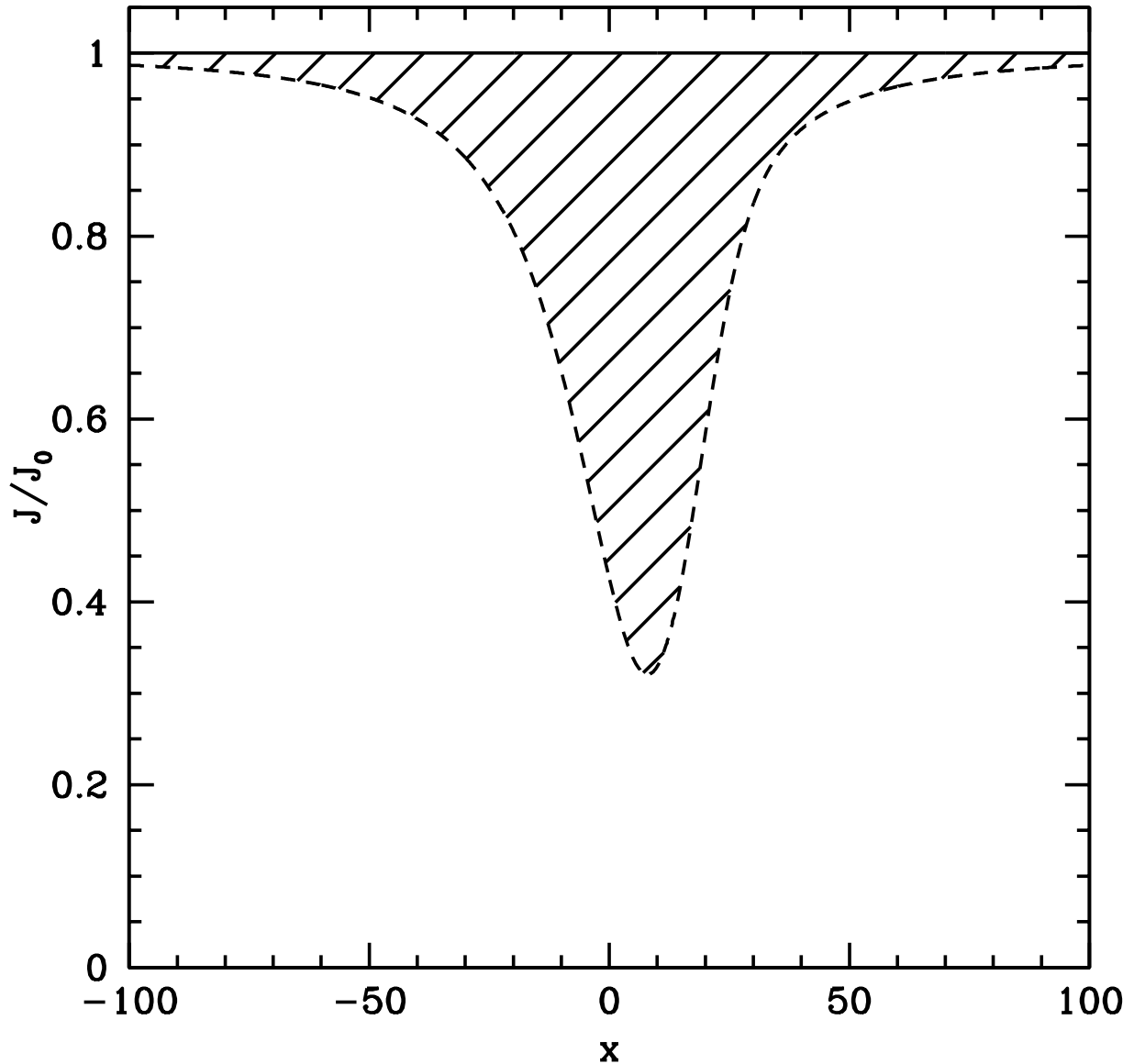


Fig. 1.— Continuum Ly α photon spectrum. Solid line marks the flat (no-scattering) limit, dash line for spectrum produced with $T=2.65$ K, $\gamma_S = 1.44 \times 10^{-6}$, corresponding to the condition of unheated gas at $z = 10$ in Λ CDM model. The area of the shaded region gives the heating rate.

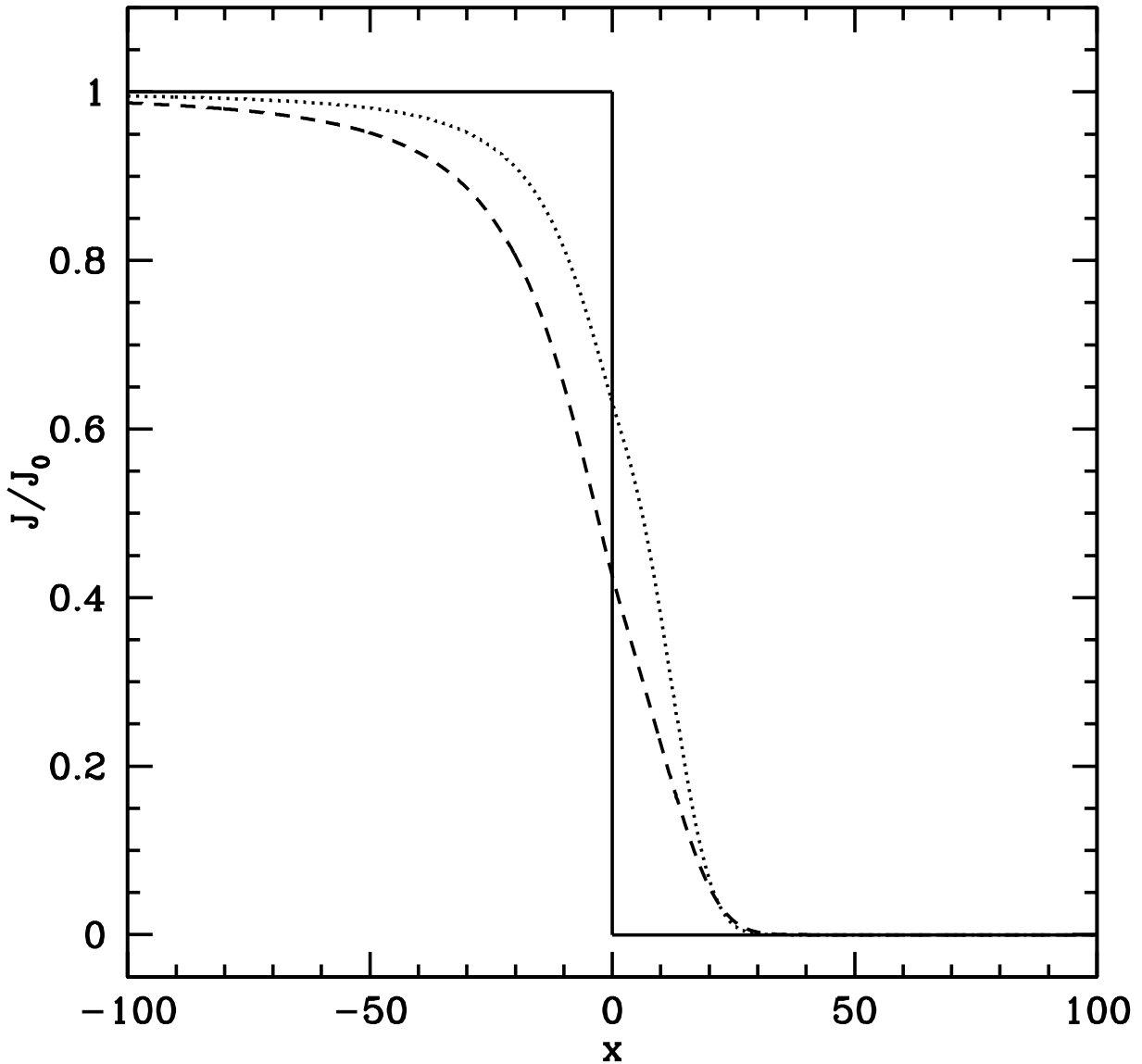


Fig. 2.— Injected Ly α photon scattering spectrum. Solid line shows the no-scattering limit. The dotted line for $T_k = 2.65$ K gas at $z = 10$ in which photon gains energy, dashed line for $T_k = 1$ K gas at $z = 10$ in which photon loses energy.

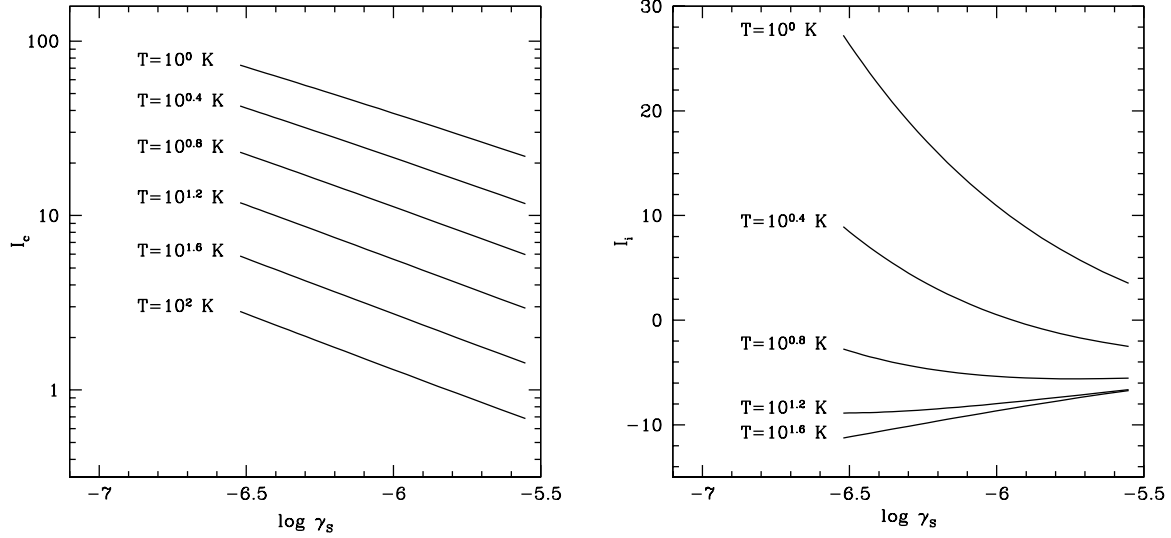


Fig. 3.— Heating rate integral I_c (left) and I_i (right) versus $\log \gamma_s$ for different temperatures.

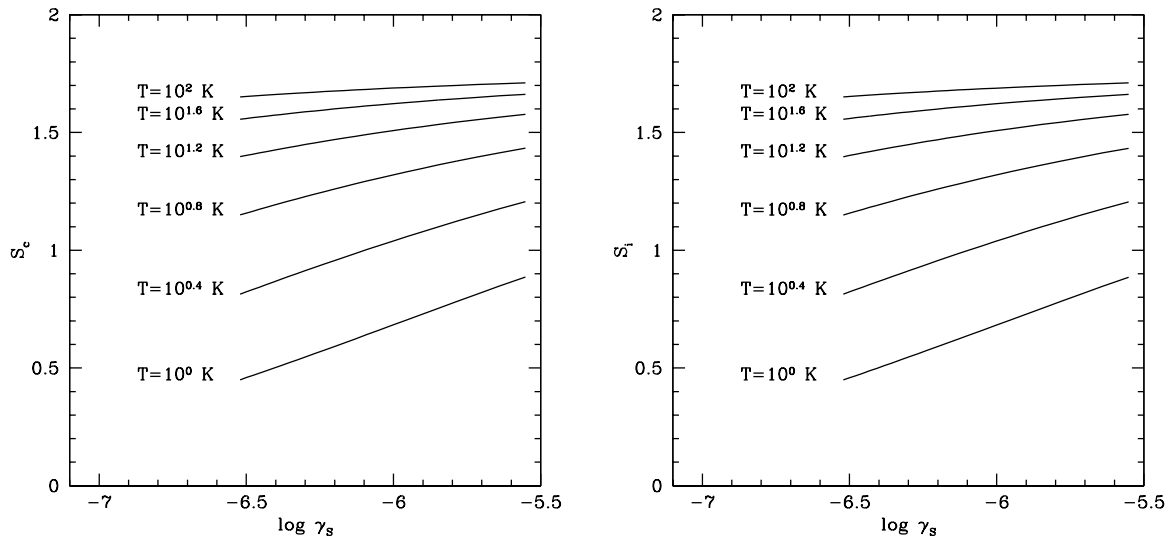


Fig. 4.— Scattering rate integral S_c (left) and S_i (right) versus $\log \gamma_s$ for different temperatures.

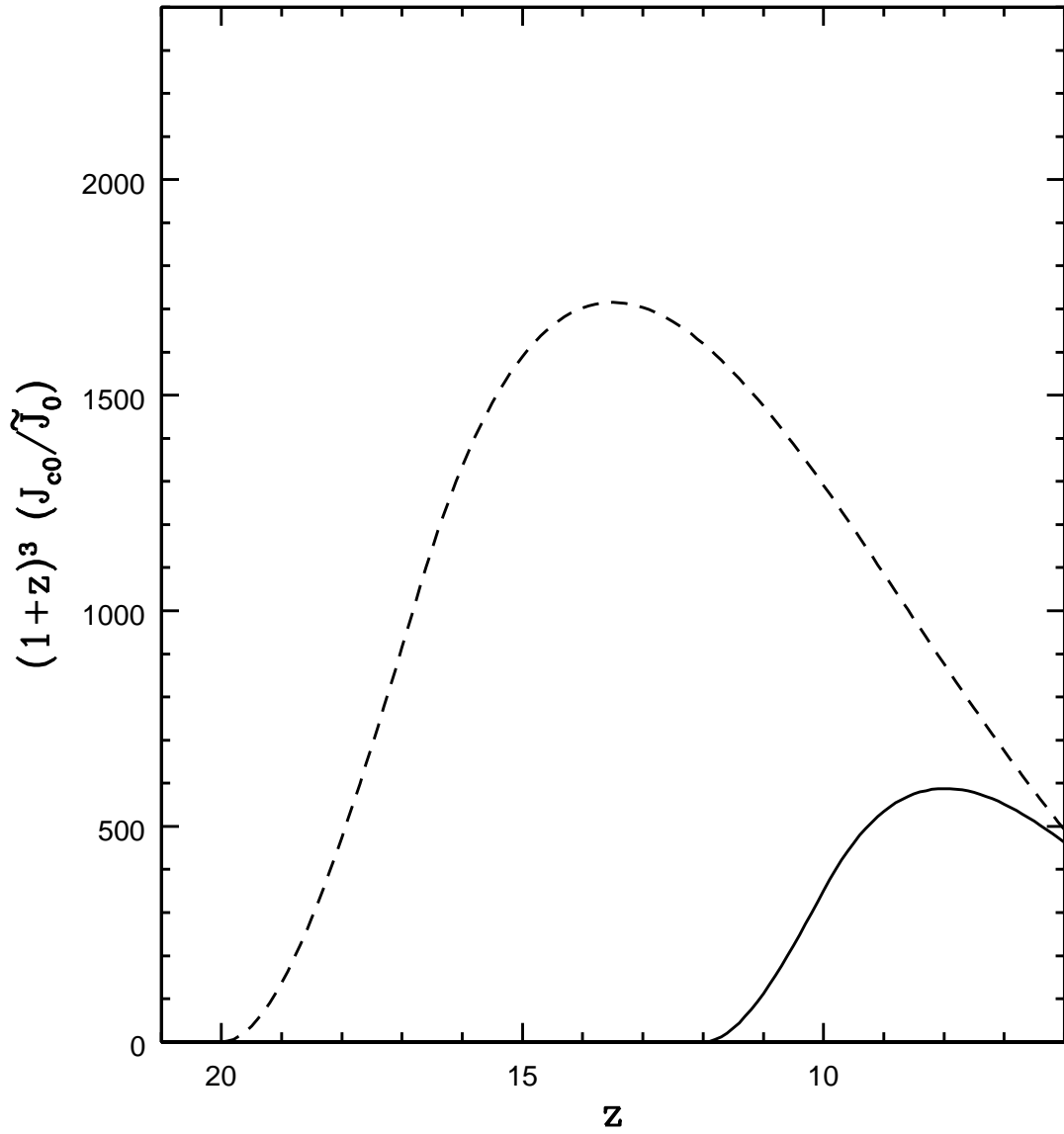


Fig. 5.— The Lyman alpha proper intensity, plotted as $(1 + z)^3 (J_{c0}/\tilde{J}_0)$, as a function of redshift. Dashed and solid curves are for $z_i = 20$ and $z_i = 12$, respectively. We also assume $J_{i0} = J_{c0}$

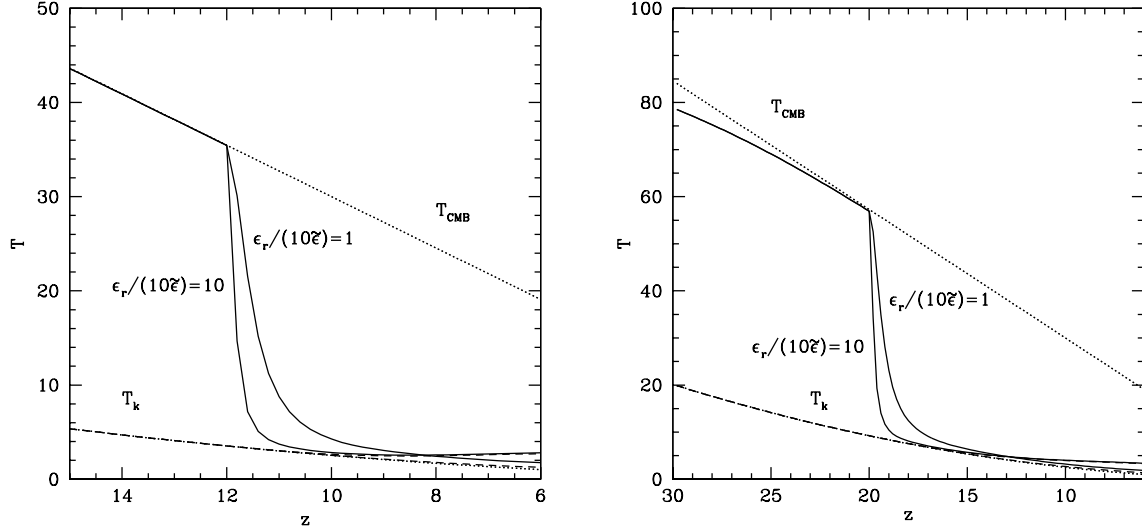


Fig. 6.— The kinetic and spin temperature evolution of the gas with only Ly α photons which increases linearly after some initial redshift z_i . The CMB temperature and adiabatic evolution of gas kinetic temperature is plotted in dotted lines, Ly α heated kinetic temperature in dashed lines, and spin temperature in solid lines. The two curves are for fudge factor $\frac{\epsilon_r}{10\epsilon} = 1$ and 10. **Left:** The “late start” scenario with $z_i = 12$. **Right:** The “early start” scenario with $z_i = 20$. Results for two Ly α emissivity models are plotted in each figure, with fudge factor $\frac{\epsilon_r}{10\epsilon} = 1$ and 10.

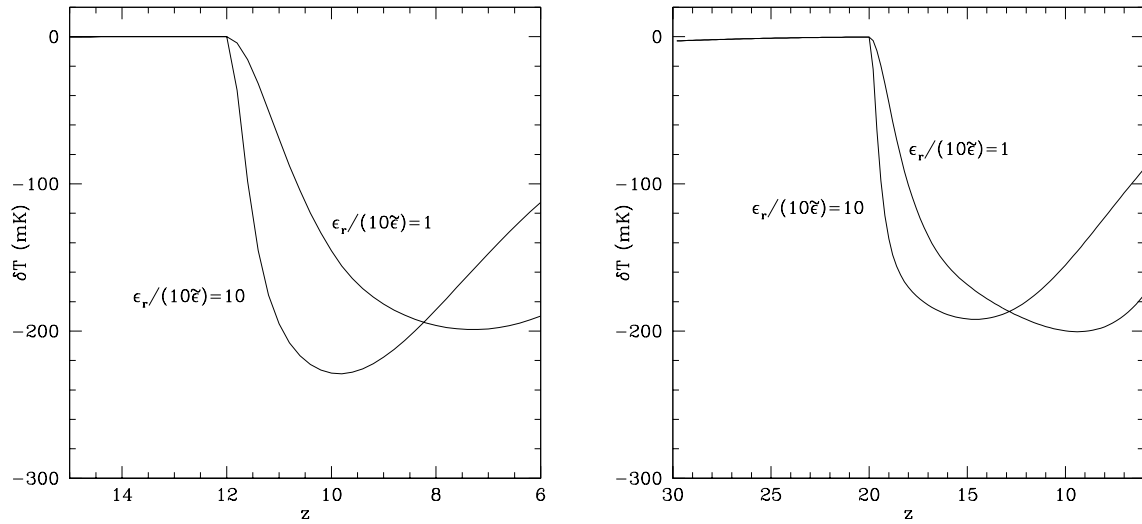


Fig. 7.— The antenna temperature difference as a function of redshift with only Ly α photons. **Left:** late start $z_i = 12$; **Right:** early start $z_i = 20$.

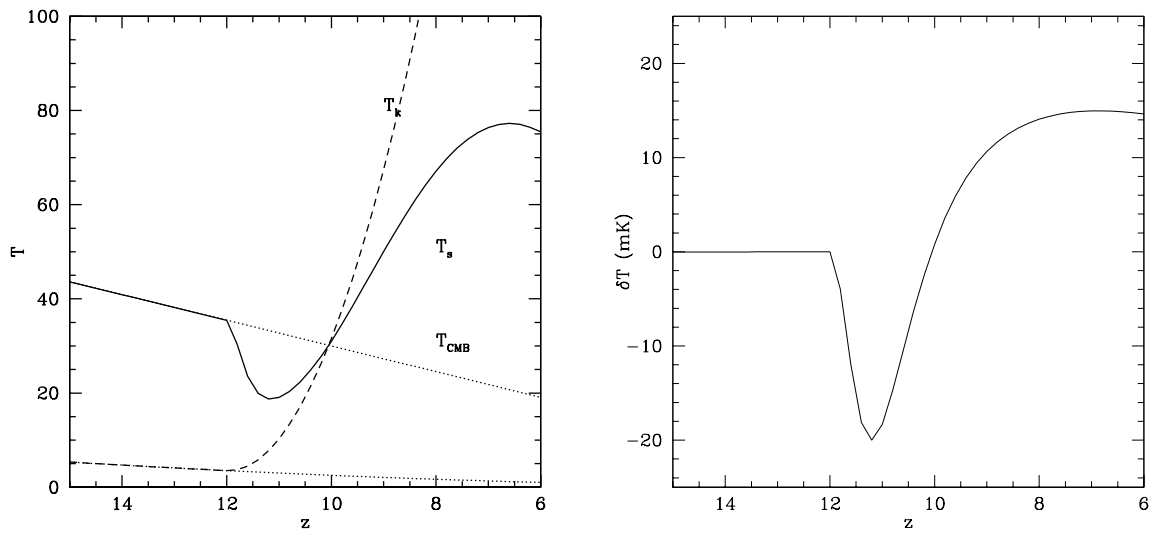


Fig. 8.— Model with X-ray heating, $z_i = 12$, $\frac{\epsilon_r}{10\epsilon} = 1$, $\alpha_x = 0.01$. **Left:** evolution of temperatures; **Right:** the antenna temperature difference.